Pollution sources and metallic elements mobility recorded by heavy minerals in soils affected by Cu-smelting (Legnica, SW Poland)

Rafał Tyszka[1],* ,
Anna Pietranik[2] ,
Beata Marciniak-Maliszewska[3] ,
Jakub Kierczak[2]

[1]Faculty of Life Sciences and Technology, Institute of Soil Science, Plant Nutrition and Environmental Protection, Wroclaw University of Environmental and Life Sciences, Norwida 25, 50-375 Wrocław, Poland

[2]University of Wrocław, Institute of Geological Sciences, pl. Maxa Borna 9, 50-204 Wrocław, Poland

[3]Laboratory of Electron Microscopy, Microanalysis and X-ray Diffraction, University of Warsaw, Faculty of Geology, ul. Żwirki i Wigury 93, 02-089 Warszawa, Poland

*Corresponding author: rafal.tyszka@upwr.edu.pl

Abstract

Heavy mineral particles are widely used in Earth science studies to show sediment provenance and weathering conditions. Such particles are particularly useful in polluted soils surrounding mining and smelting facilities because heavy minerals are common by-products of these activities and may accumulate in the soils. As such, the particles are suitable indicators of metallic element carriers and their stability in the soil environment. In this study, we analyze heavy mineral particles in two soils surrounding the active copper smelter (Legnica, SW, Poland). We show that particles associated with different smelting activities dominate the heavy mineral fraction. We note the general absence of sulfides in the fraction indicating that these minerals might have been entirely dissolved, but timing of this dissolution is uncertain (before or after deposition within soils). Currently, the carriers of potentially toxic elements are mainly secondary Fe oxides. Studies aiming at better estimation of the proportion of metallic elements contained in heavy mineral particles are needed to fully use the potential of these phases in polluted soil studies. We estimate that Pb contained in Pb-rich silicate glass constitutes <0.5% of the total Pb budget and Pb contained in secondary Fe oxides is over 1% of the total budget, but these are minimal estimates.

Keywords: polluted soil, heavy particles, metallic elements, Fe oxide, slag

1. Introduction

Heavy minerals have been widely used in sediment provenance studies for decades (Morton, 1985) and the relative stability of different heavy mineral phases has been an important tool for understanding weathering, erosion, and transport of sediments (Morton, 1984; Pettijohn, 1941). The studies of heavy minerals in sediments went through their ups and downs (Mange & Wright, 2007a), but remain an important source of information and benefit from the development of new techniques in mineralogical and geochemical studies (Hao et al., 2019; Mange & Wright, 2007b; Waroszewski et al., 2021). The application of heavy minerals goes beyond the classical provenance approach and includes geohazards (Jagodziński et al., 2012), archeology (Bong et al., 2010), and forensics (Lim et al., 2021) among others. Heavy minerals analyses have been also successfully applied to soils and provided information on elements' mobility and conditions of weathering (Table 1 – unaffected soils). In particular, studies of polluted soils located close to mining and smelting centers use heavy minerals to identify diverse sources of particles and provide information if they are prone

Table 1. A review of previous studies on using heavy minerals in soil sciences.

Soil type	Heavy minerals studied	A scientific question targeted with heavy mineral analyses	References
Unaffected soils			
Podzol	hornblende, hyperstene, magnetite, garnet	Susceptibility of different minerals to weathering	Matelski and Turk (1947)
Acid forest soil profiles (pH 4–5), galciofluvial substrate	apatite, titanite, hornblende, garnet, epidote, zircon	Documenting weathering trends	Lång (2000)
Pre-tsunami soils	pyroxene and amphibole group, opaque minerals	Soil erosion, provenance of detrital material	Jagodziński et al. (2012)
Entisols and Aridisols	non-opaque heavy minerals (zircon, tourmaline, rutile, garnet, sillimanite, and andalusite)	Provenance of detrital material	Sulieman et al. (2015)
Podzol	apatite, amphibole, epidote, hematite, hornblende, garnet, monazite, olivine, pyrite, pyroxene, titanite, zircon, rutile, and ilmenite	Determine if there is a significant contribution from these minerals to the surface geochemical signature, particularly radiogenic Pb of the soils	Carlson (2016)
Unspecified	zircon, magnetite, ilmenite, rutile and monazite	Mineral contribution to elevated contents of some elements in soils in ship-breaking yards	Khan et al. (2019)
Initial soils	transparent heavy-minerals	Documenting weathering patterns and pedogenetic processes and the addition of allochthonous material	Tangari et al. (2021)
Terra rosa represented by red palaeosol, red polygenetic soil, and two pedosedimentary complexes	epidote and amphibole groups	The provenance of initial soil material (origin of the parent material)	Razum et al. (2023)
Soils affected by mining and smelting			
The rhizosphere of industrial soils near Zn–Pb mines and metallurgical plants (Poland)	Pb, Cd, Zn carbonates, As-Pb sulphosalts, polymineralic spherules	Identification of processes in the rhizosphere leading to alteration and formation of secondary metal-rich phases, the importance of plant-root exudation solutions is stressed	Cabała, Teper (2007)
Industrial soils near mining and smelting areas	Slag particles >1 mm in diameter	Establishing slag-derived dust as a main carrier of trace elements in studied soils	Chopin and Alloway (2007)
Soils close to major smelter centers at Coppercliff, Coniston, and Falconbridge in the Sudbury area, Canada	Spherical particles composed of magnetite, hematite, Fe-silicates, sulfides, spinels, delafossite, and cuprite or tenorite	Origin and potential alteration (e.g. dissolution rates and particle-soil interaction) of spherical particles	Lanteigne et al. (2012)
Soil adjacent to mining areas	Particulate matter such as Fe silicates, spinels, sulfides, NiO, and their weathering products	Distribution of metals and metalloids in particulate matter, their formation, weathering, and mobility in soils	Lanteigne et al. (2014)
Soils within the protection zone of copper smelter (Poland)	Diverse particles associated with mining and smelting	Detecting weathering reactions in the heavy particles, implications for metal mobility	Tyszka et al. (2016)
Four different forest and grassland soils (site for the long-term experiment)	Flue dust composed predominately of arsenolite As_2O_3	Transformation of As-rich (>50 wt% As) copper smelter dust in the soil to understand As mobility and pollution risks	Jarošíková et al. (2018)
Soils developed on the slag heap after Zn–Pb smelting (Poland)	Diverse particles associated with Zn–Pb smelting	Estimating modal proportions of primary to secondary phases using automated electron microscopy	Pietranik et al. (2018)
Topsoils from hot semi-dry area (Namibia)	Diverse particles associated with mining and smelting	Automated SEM used to understand the fate/binding of metal (loids) in soils	Tuhý et al. (2020)

Table 1. Continued

Soil type	Heavy minerals studied	A scientific question targeted with heavy mineral analyses	References
Biomass-rich savanna soils, semi-arid (Namibia)	Ferric oxides, arsenolite, metal arsenates, As apatite, enargite	Understanding temperatures of mineralogical transformations and potentially toxic elements remobilization under wildfire conditions (laboratory combustion experiment)	Tuhý et al. (2021)
Soils affected by Zn mining (Lanping Pb–Zn mine, China)	Cadmium-bearing sphalerite and smithsonite	Mobility and behavior of Cd and Zn derived from smithsonite and sphalerite and their transport mechanisms in soils	Li et al. (2022)

The presented works are divided into two groups: Unaffected soils: Studies performed on natural soils and minerals.

The Table presents a few examples of such studies.

Soils affected by mining and smelting: Studies performed in areas polluted by mining and smelting.

This part is more exhaustive, aiming to include the majority of studies related to such sites.

SEM, scanning electron microscope.

to weathering (e.g. Ettler et al., 2016). Such studies are increasingly important as it has been shown that heavy minerals may be dominant metallic element carriers and, consequently, may release these elements into the environment (Yu et al., 2020). However, the diversity and complexity of heavy mineral phases in mining and smelting polluted soils (Table 1 – polluted soils) calls for better identification of these phases in local environments. In particular, the importance of heavy minerals in retaining and releasing metallic elements should be outlined in diverse locations.

In this study, we provide detailed information on heavy mineral fractions separated from two top-soil samples located close to a Cu-smelter in Legnica (SW, Poland). Heavy minerals in these soils were previously depicted by a scanning electron microscope (SEM) by Tyszka et al. (2016), who suggested that anthropogenic particles in the heavy mineral assemblage are extensively weathered and indicated them as a potentially important source of metallic elements. In this study, we follow up with quantitative electron microprobe analyses to better characterize which metallic elements might have been mobilized from heavy mineral phases and which ones are retained. We show that heavy minerals in the analyzed soils are a valuable source of information on metallic elements' mobility, and they give a new insight into the extent of pollution complementary to the classical approach based on soil chemistry and leaching tests.

2. Site Description and Historical Background

The copper smelter in Legnica was established in 1951 and started processing ore in 1953. At first, the material from the Old Copper Basin ('Lena' and 'Konrad' mines) was processed with an annual production capacity of 12,500 tons. The feeding material changed after the discovery of the new copper ore deposit in the Fore-Sudetic Monocline in 1957 by Jan Wyżykowski based on the interpretation of geological maps by Józef Zwierzycki. The processed ore came from the Lubin and Polkowice

mines and the production capacity increased in 1960 to 60,000 tons annually. Currently, the Legnica Copper Smelter produces >120,000 tons of electrolytic copper every year (https://kghm.com/). Over the years the smelter underwent modernization, also in the aspect of environmental protection. The emissions of metal-rich dusts were reduced in the 1980s and in the late 1990s, such that in 2000, the total dust emission was 96.6% smaller compared to 1995 (Monograph of KGHM Polish Copper Company, 2007; Strzelec & Niedźwiecka, 2012). Despite these modifications, the concentration of metallic elements in air and soil around the Legnica smelter remains elevated, often overstepping regulatory guidelines (Karczewska et al., 2010; Medyńska-Juraszek & Kabała, 2012; Stojanowska et al., 2020). For example, the soils immediately around the smelter that are considered the protection zone have the maximum Cu content of over 2.5 wt% (Lis & Pasieczna, 2005).

3. Materials and Methods

The soils surrounding the Legnica smelter are all classified as Cutanic Luvisols and they differ mainly in metallic elements concentration, moreover, some of the soils are used for agricultural purposes (Tyszka et al., 2016). Two soil profiles that were previously analyzed by Tyszka et al. (2016) were chosen for this study, L4 and L7 (Fig. 1), and they represent agricultural and forest soil respectively. The L7 soil profile is located close to the smelter whereas the L4 soil profile is located over 1 km from the smelter. The studied samples were taken from the horizon immediately below the litter and contained 1640 ppm Cu and 484 ppm Pb in the L7 sample and 400 ppm Cu and 164 ppm Pb in the L4 sample (for a full dataset on the chemical composition of soils see Tyszka et al., 2016). The heavy mineral fractions were separated from approximately 500 g of soil. First heavy minerals were concentrated by panning in water and then separated using the heavy liquid Na_2WO_4. The possibility of sulfide dissolution by the heavy liquid was noted and taken into account during the interpretation of results. However, based
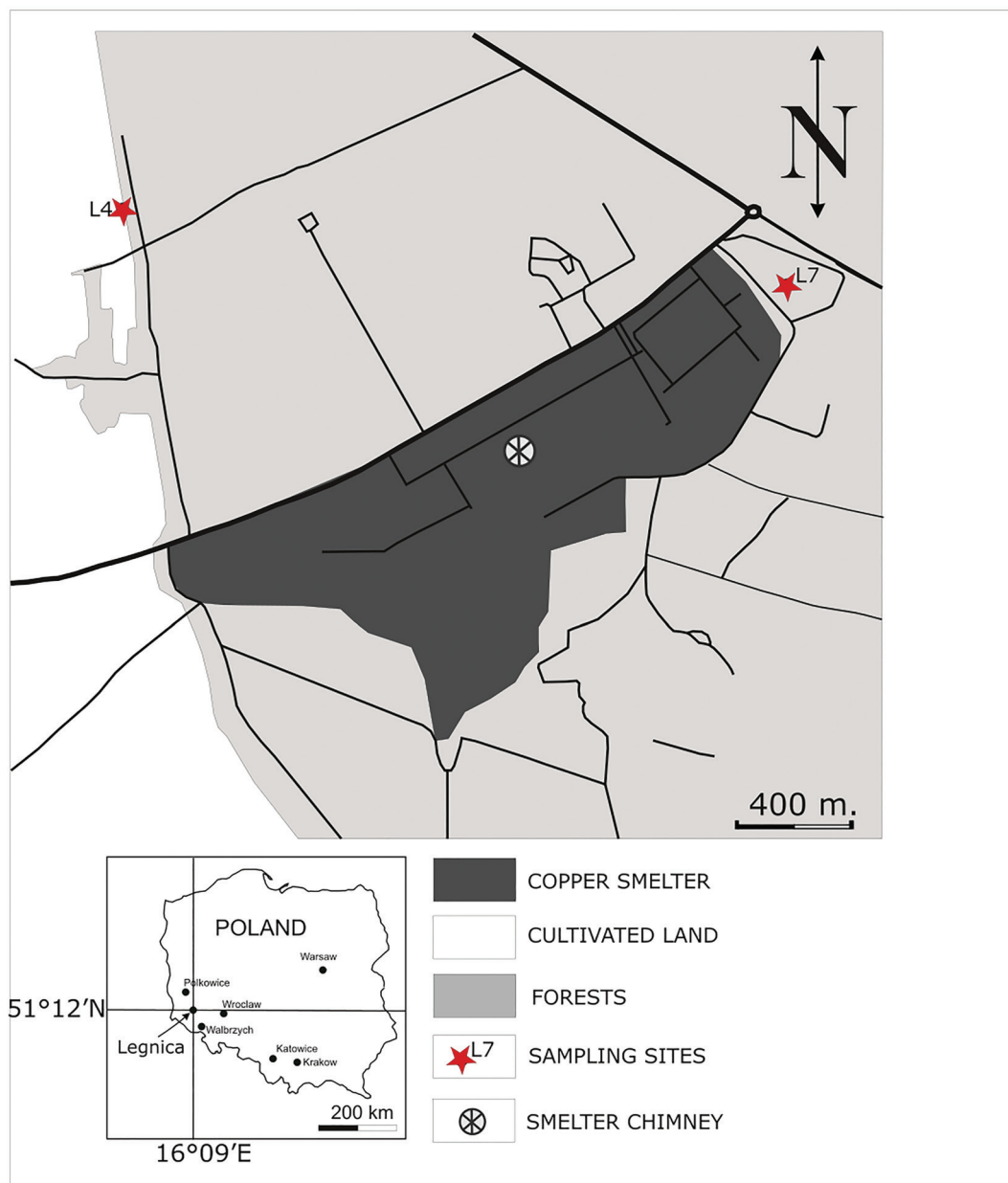
Figure 1. Schematic map of the studied area with the sampling points indicated (modified after Tyszka et al., 2016).

on complex weathering reactions observed in sulfides and concomitant secondary phases precipitation, we assumed that the sulfides were dissolved by natural processes and not during the heavy liquid separation. After separation, the phases are divided into magnetic and non-magnetic fractions using a hand-magnet. The separated heavy phases were mounted on thin sections (magnetic and non-magnetic fractions separately) and polished before they were analyzed by Cameca SX-100 microprobe at the Laboratory of Electron Microscopy, Microanalysis and X-ray Diffraction, Faculty of Geology, University of Warsaw. Specific procedures were applied to different types of minerals and a range of trace metals was determined with longer counting times to improve the detection limits. Specific procedures were used for spinels, silicates, glass, feldspars, zircons, and sulfides. Details of each protocol including information on column condition, signal condition, spectrometer setup, and standards are presented in Table S1 in Supplementary Material together with the full dataset and corresponding detection limits (Tables S2a and S2b

in Supplementary Material). The modal composition was estimated by a scanning electron microscope (SEMEDX; JSM IT-100, JEOL Ltd.) coupled with the x-act energy dispersive X-ray spectrometer (Oxford Instruments) housed at the University of Wrocław, Institute of Geological Sciences.

4. Results

4.1. Heavy minerals assemblage – general characteristics

The observed heavy mineral assemblage was diverse in both magnetic and non-magnetic fractions. The quantitative modal composition was not analyzed for this material, but clearly, different types of Fe-rich phases dominate in magnetic fraction, which was also several times more abundant by weight compared to non-magnetic one. Modal based on simple grain-by-grain calculations is given in Table 2. The Fe-rich phases were divided into two groups of Fe oxide

Table 2. Estimates of modal compositions of magnetic and non-magnetic fractions in two soil samples, based on analyses of approximately 300 individual particles. Modal proportions are based on particle counting (one EDX data point per particle, a dominating phase in the particle was chosen for multi-phase particles). The last row shows the number of particles in which potentially toxic elements (PTE) were detected by EDX (Cu, Pb, Zn, Ni, Co, V). The Fe-oxide, Fe-oxide-mix, olivine, and glass were often found in multi-phase particles, but the exact number of these was not estimated.

	L4	L7
Non-magnetic	no. grains (percentage)	
Apatite	93 (44%)	5 (2%)
Rutile	47 (22%)	53 (17%)
Zircon	41 (19%)	94 (30%)
Garnet	7 (3%)	2 (1%)
Dolomite	7 (3%)	0
Silicate glass	6 (3%)	12 (4%)
Pb-rich silicate glass	4 (2%)	0
Sulfide	4 (2%)	12 (4%)
Sphene	4 (2%)	3 (1%)
Epidote	0	65 (20%)
Fe oxide-mix	0	27 (8%)
Al-oxide	0	21 (6%)
Amphibole/pyroxene	0	22 (7%)
Total number of grains	213	316
Magnetic		
Ti-Fe phase	52 (18%)	32 (8%)
Fe oxide-mix	51 (18%)	104 (27%)
Fe oxide	37 (13%)	75 (19%)
epidote	35 (12%)	8 (2%)
Fe-Mn phase	24 (8%)	0
garnet	24 (8%)	18 (5%)
silicate glass	19 (7%)	37 (10%)
olivine	17 (6%)	41 (11%)
amphibole/pyroxene	15 (6%)	40 (10%)
sulfide	6 (2%)	7 (2%)
chromite	4 (1%)	16 (4%)
Ca ferrite	4 (1%)	7 (2%)
Total number of grains	288	385
Phases with PTE	20 (7%)	46 (12%)

PTE, potentially toxic elements.

(SEM-EDX analyses showed only Fe and O spectra), and Fe oxide-mix (SEM-EDX spectra were dominated by Fe and O, but also showed other elements). The detected assemblages were generally similar between L4 and L7 profiles for magnetic fraction, but the L7 sample contained a higher proportion of Fe oxide and Fe oxide-mix phases, as compared to the Ti-Fe phase (ilmenite and titanomagnetite) that dominated in L4 sample. Also, 12% of particles showed Cu, Pb, Zn, As or Co signals in SEM-EDX spectra in L7, whereas only 7% of such phases were found in L4. The main difference for non-magnetic fraction was abundant apatite in agricultural soil L4, which was absent in the forest soil L7 sample. The phase most probably represented diverse fertilizers.

Some particles were monomineral (garnet, ilmenite, zircon, rutile, dolomite), but many of them were complex, and composed of several phases. The complex particles could be classified as natural or anthropogenic. The first group included rock fragments (mainly amphibolite), whereas the second group included slag fragments. Sulfides were rare and always showed signs of weathering. Dolomite was probably also related to mining and represented gangue rock or could represent a flux. This study was particularly focused on the particles that may have contained elevated contents of potentially toxic elements and they were considered also, in the context of their stability (i.e. is alteration visible or not). Such particles included Fe oxide and Fe oxide-mix, sulfides, slag fragments and Pb-rich silicate glass. Particles containing anthropogenic zircon were also observed.

Based on SEM analyses the Fe oxide-mix group can be further divided into three subgroups depending on the additional elements, which the particles contained: (1) approximately 50% of Fe-mix-oxides contained only elements such as Si, Al, Mg, Ca, (2) in 25% of particles, in addition to these elements sulfur was detected, and minor elements including potentially toxic ones may or may not have occurred, and (3) in 25% of particles, variable elements were detected depending on the phase (e.g. Cu, Pb, Zn, Co, V, Mn, Ni), but no sulfur.

4.2. Iron oxide phases

This group is strongly diversified in terms of grain size, morphology, and composition (Fig. 2) with Fe always being the dominating component. In this group, we included phases with Fe [wt%] content exceeding 40% and divided them into two sub-groups based on chemical composition as analysed by electron microprobe: Fe oxides with high totals (mostly exceeding 90%) and Fe oxides with low totals (mostly within the range 65%–90%, Fig. 3A). The lower totals were most probably a combination of several factors such as the presence of hydroxyl group, Fe^{3+}, or porous structure. This division did not reflect the real variability in Fe oxide phases that may include Fe oxides *sensu stricto* such as magnetite ($Fe^{3+}_2Fe^{2+}O_4$) and hematite ($Fe^{3+}_2O_3$), as well as ferrihydrite ($Fe^{3+}_2O_3 \cdot 0.5(H_2O)$) and Fe oxyhydroxides ($Fe^{3+}O(OH)$ polymorphs such as goethite, lepidocrocite, feroxyhyte, and akaganeite). It is difficult to assign analyses of particular Fe oxides to a mineral name, firstly because they represent a mixture of different Fe phases, but also because admixtures of other elements (Si, Al) contaminate the analyses. The other elements could indicate the presence of unweathered minuscule silicates or silica and Al oxyhydroxides precipitates from secondary fluids. Alternatively, they could be components sorbed or formed within the Fe oxides after their deposition in soils. Therefore, a possible assumption is that the first group is mostly represented by magnetite and hematite, whereas the second group is dominated by various Fe oxyhydroxides and/or ferrihydrite. The first group contains spherical particles (Figs. 2A and 2F), angular monomineralic fragments (Figs. 2B, 2C, 2F), larger porous particles (Figs. 2B, 2C, 2G),
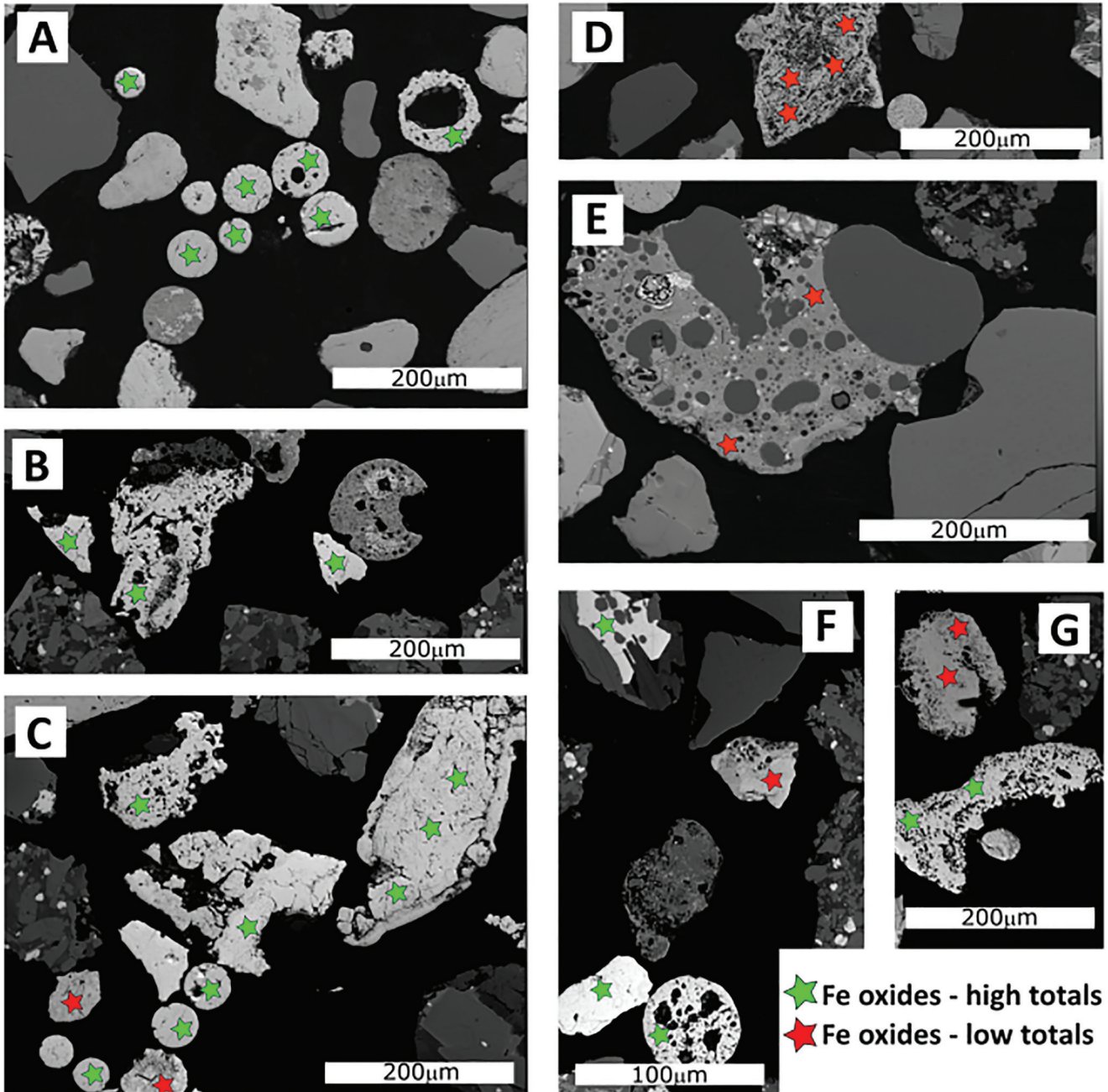
Figure 2. Back-scattered electron images of two types of Fe oxides identified in this study. The two groups are identified based on their chemical composition and a distinct character of the groups is reflected by low and high totals of the electron microprobe analyses. These two groups are indicated in the Figure with different colors of the stars. (A) numerous spherical particles composed entirely of Fe-oxide with high totals; (B) small angular monomineralic fragments (i) and a larger porous particle (ii); (C) spherical particles (i), larger porous particles (ii) and anhedral, strongly porous grains (iii), (D) strongly porous grain with low total; (E) a Fe-rich glass-like material containing quartz grains; (F) a skeletal grain within a slag fragment (i), anhedral, strongly porous grains (ii), small angular monomineralic fragment (iii) and a spherical particle (iv); (G) larger porous particles.

and grains within complex slag fragments (Fig. 2F). The second group is mostly represented by anhedral, strongly porous grains (Figs. 2D, 2F, 2G). Uncommon occurrences include a Fe-rich glass-like material containing quartz grains (Fig. 2E). The two groups differ in chemical composition, the low-total group contains higher concentrations of other elements, most notably Si (Fig. 3B) compared to the high-total group, which is probably due to the presence of admixtures with sizes below the resolution of the microprobe beam. Also, metallic elements such as Pb and Cu occur usually above the detection limits of electron microprobe in the low-total group and are below detection in high-total Fe

oxides (Figs. 3C and 3D). Based on electron microprobe analyses, sulfur was detected in 24 out of 41 analyzed low-total Fe oxide phases.

4.3. Slag fragments

This group included angular fragments composed of several phases and it was strongly diversified in terms of phase composition and texture. Figure 4 shows examples of six slag fragments and each of them contains different phases with variable metallic elements contents. Spinels and silicates are common phases, but they differ in composition between the slag fragments;
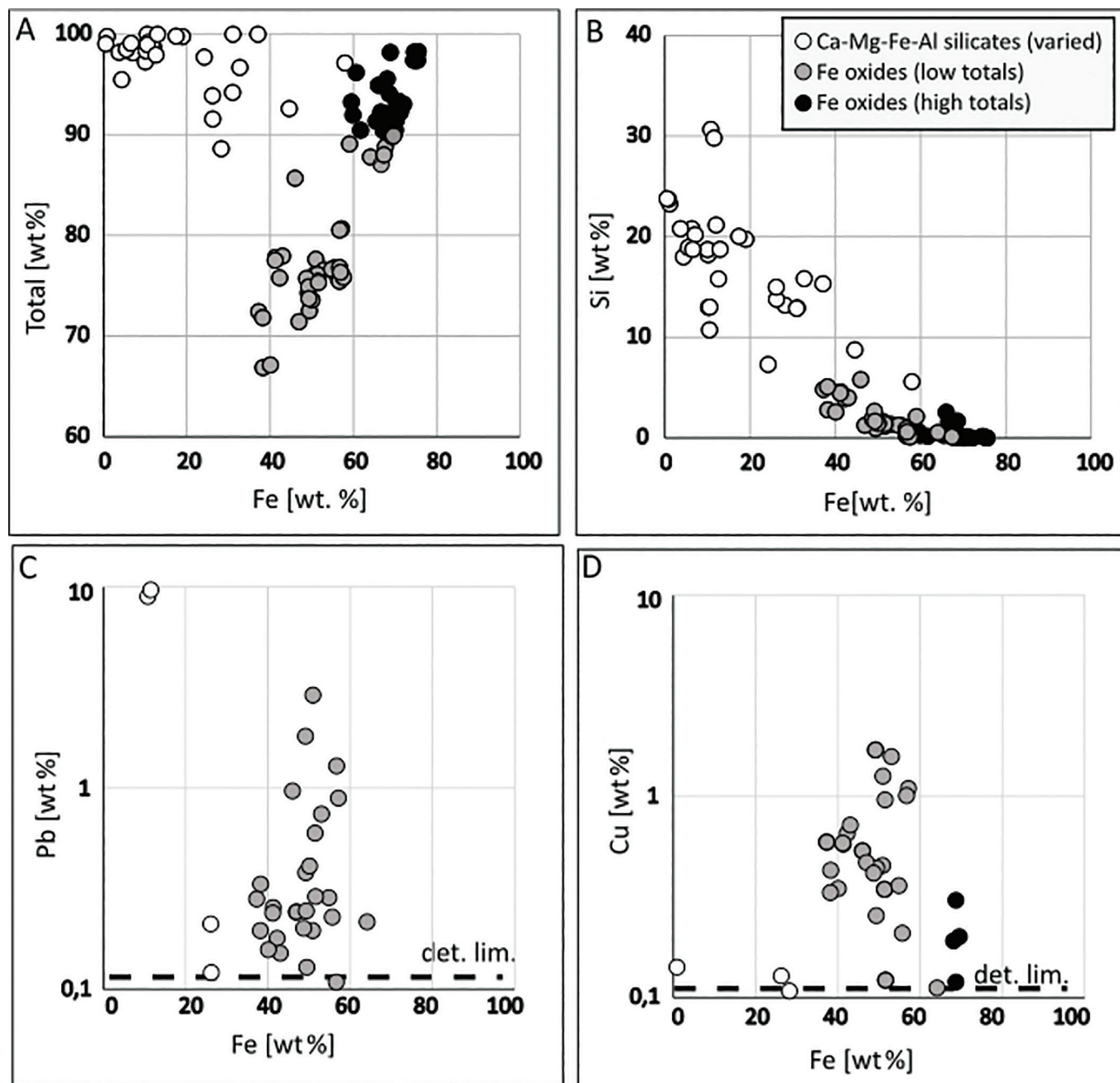
Figure 3. Composition of two types of Fe oxides (low and high totals) and Fe-rich silicates. The detection limit of electron microprobe analyses is indicated (det.lim.), phases shown in (A,B) and not in (C,D) have Pb and Cu contents below the detection limit.

also, glassy material is strongly compositionally diverse (Figs. 4A and 4B and Supplementary Material). For example, Pb content in slag glass is either below the detection limit (white symbols in Figs. 4A–4C), reaches 10 wt% (red star, Fig. 4B), or is as high as 40 wt% (Fig. 4D). Some fragments do not contain Cu, Zn, and Pb, but show elevated contents of other elements such as V (Fig. 4A) or Ba (Fig. 4E). Also alteration features range from extensive (rims in Figs. 4A and 4E) to absent (Figs. 4B–4D).

4.4. Pb-rich silicate glass

Pb-rich silicate glass occurs in both profiles and consists of silica (25–50 wt%), alumina (5–10 wt%), and Pb (41–68 wt% as PbO). It also contains Fe, K, Ca, and Na and traces of Mg, Ti, Zn, and Cu. The fragments show signs of alteration that form discontinuous

rims with low Pb contents around the fragments and a similar reaction propagates along the fractures (Fig. 5A) or irregular tunnels (Fig. 5B). The Pb-poor rims reach the thickness of 25 μm in L7 compared to 15 μm in L4. Generally, the composition of the glass can be divided into three groups related to the intensity of the alteration. Group 1 is represented by the primary glass and is characterized by high Pb contents (>50 wt% PbO) and inverse correlation of Pb and silica. Closer to the rims, patches characterized by the uneven appearance and darker color in the Back Scattered Electron (BSE) image occur (Figs. 5A and 5B). They contain less Pb and more Si, Al, and K than the primary glass. The outermost rims are Pb-poor and have scattered Si and other element contents (Figs. 5C and 5D); some of the analyses also have low totals, suggesting a hydrated composition. The scattering is expected as evident from SEM
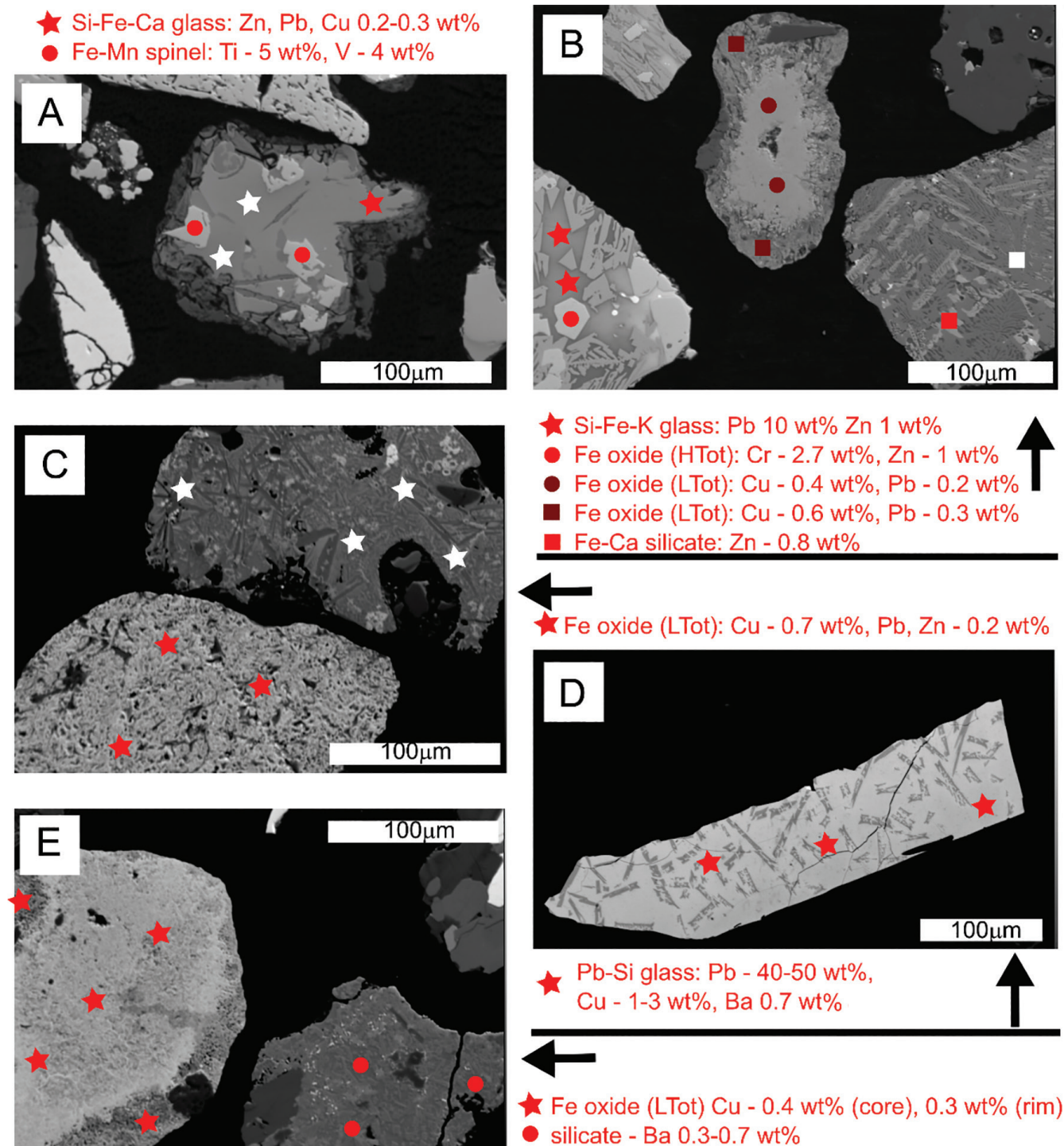
Figure 4. Diverse slag fragments observed in the studied soils, the contents of chosen potentially toxic elements measured by electron micro¬probe are indicated for each fragment. White symbols show places where such elements were below the detection limit. (A) slag dominated by glass containing euhedral spinels (lighter), and silicates (darker), weathering proceeds along rims and cracks, (B) two slag fragments containing glass and different phases, (i) not weathered, (ii) slightly weathered, the third fragment (iii) is strongly weathered and could represent slag or other anthropogenic material, (C) two slag fragments (i) slag showing extensive replacement by Fe-oxides, (ii) slightly weathered slag dominated by crystalline phases spinels and silicates, (D) unweathered slag dominated by Si-Pb glass containing skeletal crystals of Pb-poor silicate, (E) weathered slag fragmnents, (i) slag showing extensive replacement by Fe-oxides, (ii) slag dominated by Ba-silicates.

compositional mapping (Figs. 5E–5G). Clearly, low-Pb rims are composed of several inter-mixed phases.

4.5. Other particles rich in metallic elements

Other particles containing metallic elements are sulfides (mostly chalcopyrite, bornite plus rare galena) and metals (predominately Fe, but alloys of other metals were also found e.g. Sn or tiny Pb droplets).

As seen in Table 2 these phases are very rare (metal alloys were not detected by particle-by-particle counting), but they may contain high concentrations of metallic elements other than the main constituents. Chalcopyrite contains Ag, whereas bornite Pb, Zn, Co, and Ni. Iron alloys contain over 0.1 wt% of Ag and As (Table S2a and S2b in Supplementary Material). Sulfides are commonly surrounded by altered rims composed mainly of Fe oxides and silica (probably amorphous
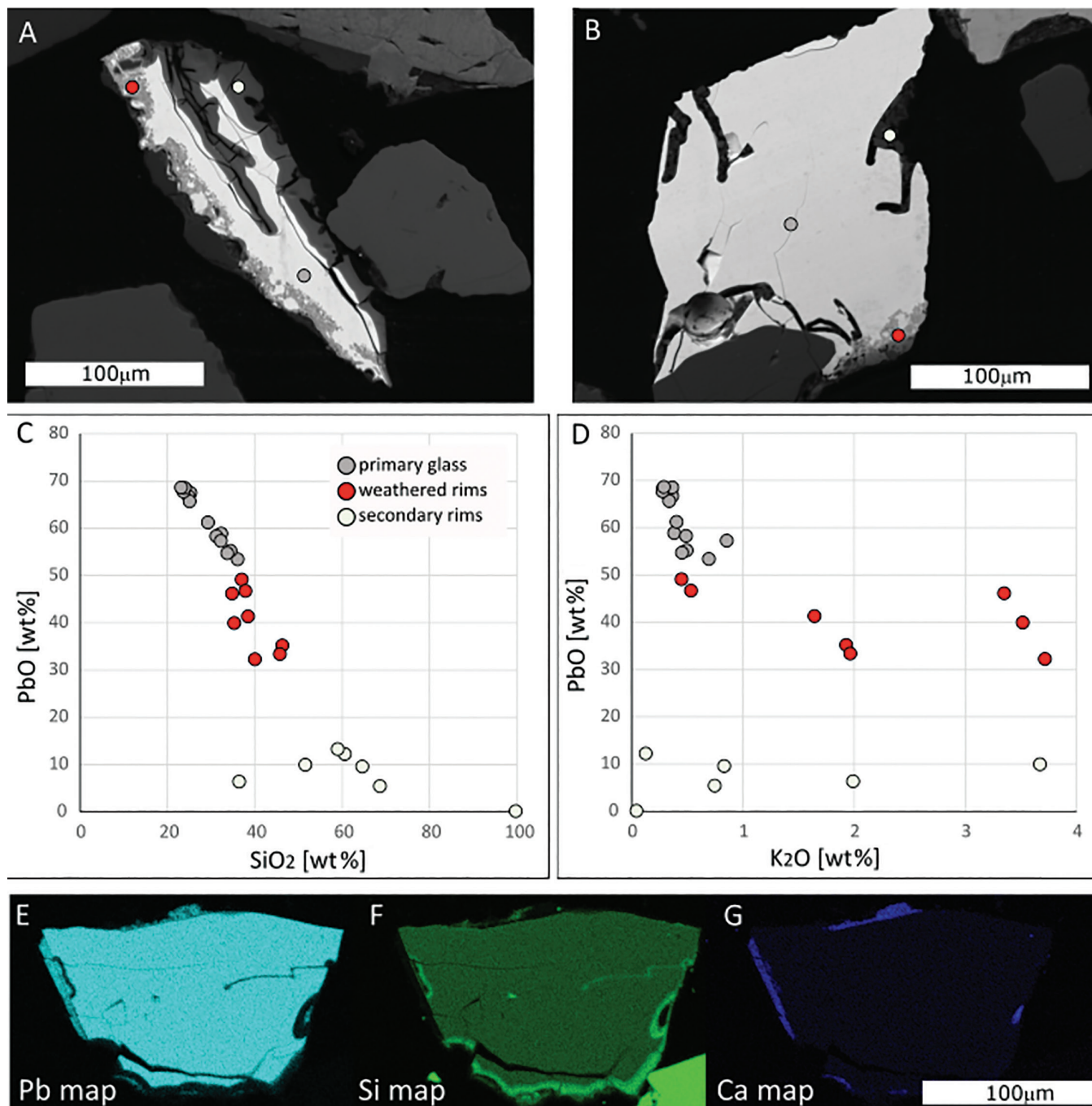
Figure 5. (A,B) Back-scattered electron images of Pb-rich silicate glass showing weathered rims. (C,D) Electron microprobe analyses shown for all analyzed particles in this group, the analyses are divided into three groups based on the observed extent of weathering in BSE images. The analytical points belonging to each group are shown in (A,B). (E–G) EDX maps for Pb, Si, and Ca of a Pb-silicate glass particle. The relative color intensity scale shows the element-rich (bright) and element-deficient (dark) parts of particles.

silica precipitate), but also containing other metallic elements such as Mn and Pb. The chalcopyrite grain shown in Fig. 6A is altered along rims and fractures, some Fe oxide patches are observed also within the grain, and precipitation of Fe-Mn oxides is observed along the fractures (Fig. 6A). Within the more porous weathered fragments other elements such as Pb, Co, As, P and Si were also detected (only EDX analyses exist for this particular grain). In contrast, the chalcopyrite shown in Fig. 6B is characterized by a thin rim composed mostly of Fe oxide, but also containing some W. As we used sodium polytungstate to separate heavy phases the liquid might have reacted with sulfide particles, this was probably the case for the grain in Fig. 6B. However, as other grains show extensive alteration

with no W addition, we conclude that the majority of sulfides are altered by natural processes.

4.6. Anthropogenic zircon

Spherical particles and breccia-like fragments composed of fragmented zircon and Zr-rich glass (Fig. 6C) constitute approximately 1%–5% of the zircon particles found in the studied soils. The composition of this anthropogenic zircon is indistinguishable from the natural one analyzed in this study. The glass in breccia-like fragments is composed of SiO_2 (73 wt%), Na_2O, and Al_2O_3 (7–8 wt% each) and contains up to 5 wt% of ZrO_2, interestingly Ce contents above the detection limit were also measured (approx. 1500 ppm,
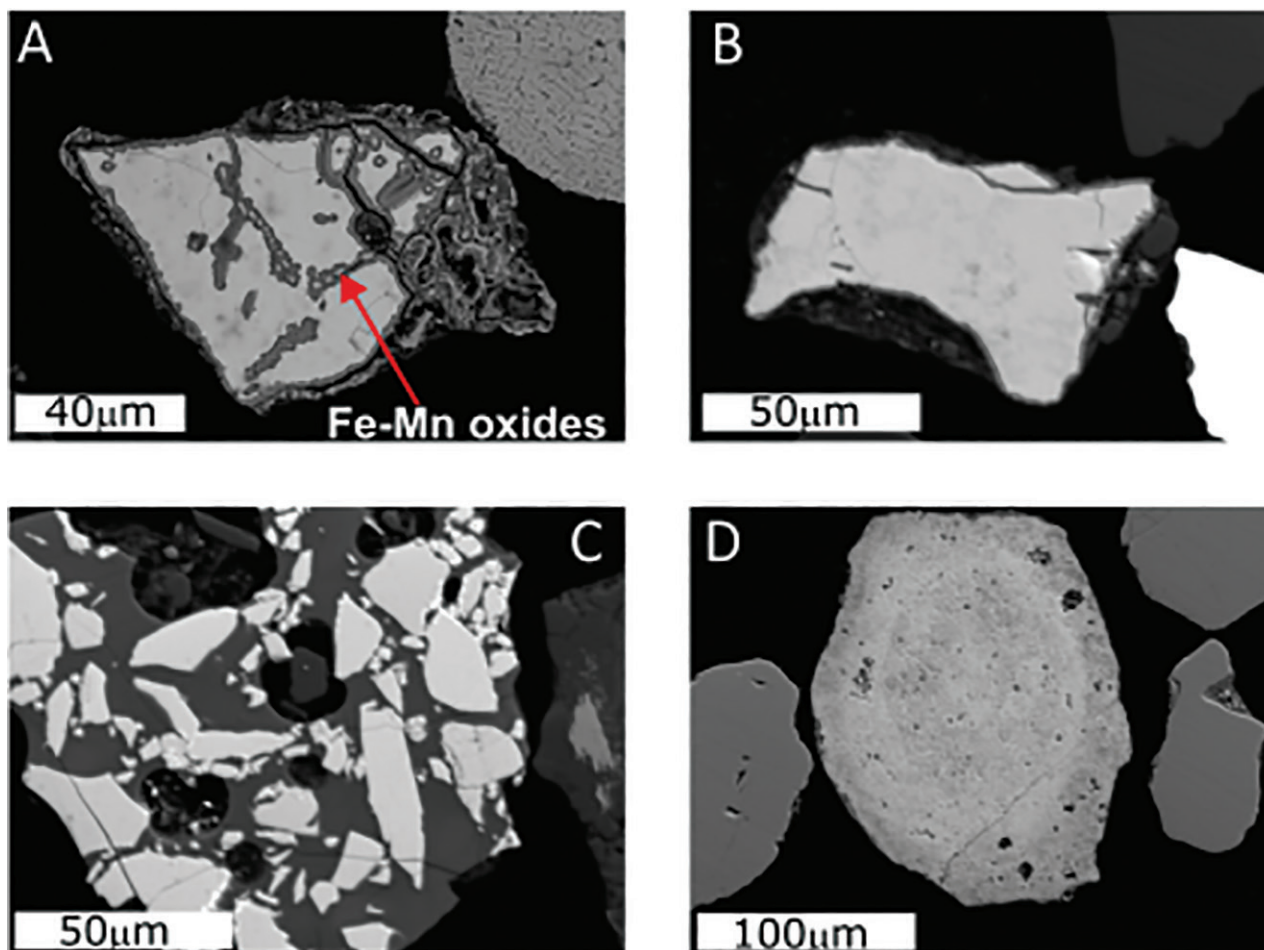
Figure 6. Back-scattered electron images of minor phases occurring in the studied soils: (A) chalcopyrite with well-developed weathering features, the secondary products include Fe oxides with Mn and Co, and silicates, (B) chalcopyrite with thin weathered rim, (C) zircon breccia in Zr-rich glass, and (D) phosphate grain.

Table S2b in Supplementary Material). The breccia-like fragments can be remnants of abrasive materials used in the smelter (e.g. Cho et al., 2008).

4.7. Phosphates

The main difference between agricultural and forest soil is the presence of abundant apatite grains in the former. The grains most probably represent a phosphate fertilizer and provide insight into its reactivity. Several types of apatites were noted with the dominance of oval, porous grains (Fig. 6D) or large angular fragments with no porosity. The oval grains were analyzed in this study showing Pb and Cu contents slightly above the detection for a few grains (Table S2b in Supplementary Material). Interestingly, high metal contents are limited to minuscule grains, usually observed within pores. It is unclear if these are newly precipitated or mechanically included.

5. Discussion

5.1. Insight into the sources of anthropogenic material

As was noted by studies dealing with soils polluted by mining and smelting activities (see Table 1 and references within) the heavy minerals in soils may originate at

different stages of mining and smelting procedure. Ettler et al. (2016) grouped the grains based on their size, phase composition, and morphology into five categories, which were related to diverse sources and similar sources may be envisaged for particles analyzed in this study:

(1) Particles related to mining operations or derived from mine tailings. They are angular, 5–150 μm in size, and composed of ore and gangue rock minerals (Ettler et al., 2016). In this study, sulfides and dolomite may be associated with this group.
(2) Spherical particles 20–150 μm in size related to emissions from the smelter. Such particles are common in the studied soils and are mostly composed of Fe oxide, sometimes silicates, or rarely zircon. These particles are usually not weathered and therefore seem stable in the soil environment near the Legnica smelter.
(3) Highly weathered metal-rich particles formed in the flue-gas cleaning system. Not many similar particles that can correspond to this group were identified in this study, but some Fe oxides with low totals may represent such grains.
(4) Irregular grains of smelter slags, blown from the disposal sites. This type of particles is common in the studied site and they are highly diverse including several types of slag and glasses. The most interesting is the Pb-rich silicate glass that

occurs in both studied profiles and shows signs of weathering. Sulfides may also belong to this group.

(5) Secondary precipitates sticking other particles together. Such particles were also observed in this study (Fig. 2E). Some grains composed of Fe oxides with low totals may also be considered as belonging to this group.

Among the studied phases Fe oxides are the most common and not straightforward to classify. They could be derived from several smelting-related sources or could be formed within the soil as secondary minerals or precipitates. Some of them have a spherical morphology and low porosity and can be regarded as particles emitted from the smelter formed during rapid cooling of the liquid oxide (Fig. 2A). Similar particles were observed in soils surrounding the Zn-Pb smelters near Olkusz (Cabała & Teper, 2007). Some Fe oxides may occur in slag fragments (Fig. 4), which may be rich in primary magnetite, a common phase formed during rapid cooling and transformation processes within smelter and converter facilities, (Lanteigne et al., 2012). However, the majority of the particles have diverse sizes and irregular shapes (Figs. 4C and 4E). These Fe oxides are characterized by porous structures that may suggest that they represent slag fragments or sulfides that were oxidized to diverse Fe oxides when they were deposited in soils. This is consistent with experiments that simulated the reaction between slag and acidic water leading to the formation of Fe oxide and silica gel (Tyszka et al., 2021). We suggest that similar products of intense weathering of smelter-derived particles are common in the studied soils. However, particles of Fe oxide with low totals may also have been formed naturally in soils by precipitation and it is difficult to distinguish them from the products of slag and sulfide weathering.

The analyzed assemblage may be compared to phases emitted recently from the Legnica smelter that were deposited on spider webs (Trzyna et al., 2022). Anthropogenic silicates were observed both in our study and that of Trzyna et al. (2022). The authors noted also a high proportion of sulfides in fractions <2.5 μm and the general absence of sulfides in fractions >10 μm. The sulfides were rare in our study, however, we analyzed mostly fractions >10 μm. The sulfur signal was detected in at least 50% of Fe oxides with low totals, which may indicate that the sulfides were commonly present in the soil, but were weathered and replaced by Fe oxides. However, the adsorption of sulfates present in soils cannot be excluded. Also, Fe oxides were rare in the study of Trzyna et al. (2022) and attributed mostly to erosion of local constructions (rail tracks, industrial metal structures). The abundance of such particles in the soils and their general absence in recent air-deposited material may favor their precipitation in the soils. However, the differences between phases from recent air deposition and those in soils may be also due to the change in the phase composition of emitted material with the soil containing particles emitted over 70 years of the smelter activity. Summarizing, the origin of Fe oxides is complex and possible origins include anthropogenic particles, secondary products after anthropogenic particles weathering and soil precipitates. Establishing more exact proportions between the particles of diverse origin requires more detailed in-situ analyses of phases coexisting within a single Fe oxide particle.

5.2. Insight into metallic element mobility

So far, heavy minerals in polluted soils have been used to detect possible weathering reactions and estimate the stability and mobility of metallic elements in soils affected by mining and smelting (Table 1). A similar approach can be applied to particles analysed in this study. For example, we observed that Pb-rich silicate glass is readily weathered potentially releasing a considerable amount of Pb. On the other hand, sulfides are characterized by more complex reactions. Some of them are slightly weathered (Fig. 6B) and some show more extensive weathering (Fig. 6A). The experiments performed on Cu-slags showed preferential weathering of glass compared to sulfides in alkaline conditions (pH >7, Potysz et al., 2018). However, the soils around Legnica are slightly acidic (pH 5.6–6.5) to near-neutral (6.6–7.2) and not alkaline (Hołtra & Zamorska-Wojdyła, 2020), which should not promote extensive glass weathering and also stabilize sulfides. Therefore, the range of observed weathering features probably reflects the complex nature of the soils. As anthropogenic material has been released from the smelter for over 70 years, it probably weathered at different rates and conditions at different times.

As noted above Fe oxides may be a product of extensive weathering and they may also contain metallic elements such as Pb, Cu, and Zn. Tyszka et al. (2021) showed that secondary Fe oxides may rapidly form in slag material in experimental conditions under acidic pH (simulated acid rain conditions). Extensive weathering is not expected in near-neutral soil, but the particles may have been already weathered and transported from slag disposal sites or be affected by fluctuating pH e.g. after heavy rains with more acidic pH. Legnica lies in the area, where pH in the period 2002–2019 is generally low, in the range of 4.8–5.2, compared to other regions in Poland (https://powietrze.gios.gov.pl/pjp/maps/chemistry/precipation). The longer timespan of pH measurements can be accessed for the Śnieżka mountain from the European Monitoring and Evaluation Programme (Tørseth et al., 2012). It is evident that the precipitation was more acidic with pH values often below 4.0 in the early 90's and it is possible that even lower values were noted before, in the period commonly affected by acid rains in Poland. Such a situation may be compared to the Świętochłowice slag dump, which contained high amounts of fine-grained weathered material composed mostly of Fe oxides formed after long-term deposition of slag affected by recurring acid rains (Tyszka et al., 2014). The elevated contents of elements such as Cu, Pb, and Zn are probably due to the presence of secondary phases that trap these elements or minuscule remnants of primary phases (sulfides). Unfortunately, the resolution of both SEM-EDX and electron microprobe used in this study is too low to recognize individual phases in complex Fe oxides. Further research by field emission

SEM may give better characteristics of the phases and their potential mobility. However, despite the difficulties of assigning elevated contents of metallic elements to a particular phase, the complex Fe oxides must be considered as the main carrier of smelter-derived pollution currently residing in the studied soils.

5.3. Insight into environmental monitoring

This study and others shown in Table 1 confirm the usefulness of heavy minerals to characterize pollution sources and the fate of the particles derived from mining and smelting. However, the vital information on the general pollution in the area should assign metallic elements to particular phases in the context of the whole soil metallic elements budget. This can be done if the weight proportion of heavy mineral fraction in the soil sample is estimated. A good example of quantitative studies done in a similar context of anthropogenic particles accumulated in soils and sediments is research on glass microspheres. It was shown that the number of microspheres differs between their depositional sites that delineated the routes of their preferential transport (Gałuszka & Migaszewski, 2018; Migaszewski et al., 2022). These conclusions were only possible because the total number of microspheres was calculated per kilogram of the sample. Such an approach was not applied in this study, but rough estimates can be done based on approximate modal proportions and the number of analyzed grains. For example, assuming that Pb-rich glass was fully separated within a non-magnetic fraction and most of the fraction was mounted, we expect 10–15 grains of Pb-rich glass per 500 g of material used for heavy mineral separation. Further assuming a spherical shape and 100 μm radius of the particles as well as Pb content of 50 wt% and density around 5 g/cm^3 (estimated after Kacem et al., 2017), it can be calculated that <0.5% of the total Pb budget is contained in these particles. On the other hand, Fe oxide particles are much more abundant (estimated at several thousand particles per 500 g soil) and they may contain >1% of the total Pb. Taking into account that these are probably minimal estimates the calculations show that heavy minerals may contain an important part of the metallic elements budget, but time-consuming methods are required to estimate it properly.

6. Conclusions

Elevated contents of metallic elements occur in heavy mineral particles originating from various smelting activities in the Legnica smelter. They were accumulated in nearby soils and their diversity probably reflects 70 years of the smelter activity. Most of the anthropogenic particles can be attributed to diverse sources within the smelter, but weathering of construction structures, and fertilizers also contribute material to the heavy mineral fraction. Both heavily weathered and unweathered anthropogenic particles occur in the soil, which also may reflect changing conditions over decades of their accumulation. The most spectacular weathering is observed in sulfide and on Pb-rich silicate glass particles that are dissolved releasing Cu and Pb into the soil solution. Metallic elements such as Cu, Pb, and Zn occur also in Fe oxides with low totals, which may be a product of silicate and sulfide weathering and maybe the main phase that retains the metallic elements.

Altogether heavy minerals provide important information on metallic elements distribution and mobility in polluted soils, however, some improvements may be introduced. Discrepancies between the phase assemblages observed in soils and those deposited from air suggest diversities between different size fractions. Dividing heavy minerals in different size fractions or better control of particle sizes e.g. by using automated SEM analyses (Pietranik et al., 2018; Tuhy et al., 2020) may provide additional information. At the same time, better resolution for the phase observations is promising, especially for complex Fe oxides that are composed of intermixed primary and secondary phases. Finally, an approach to extracting quantitative information should be sought e.g. by better estimation of the weight proportion of heavy minerals and by counting the total number of particles. Rough calculations done in this study show that heavy minerals may constitute an important fraction of the whole metallic elements budget, but confirming this requires careful and meticulous analyses mimicking those done for glass microspheres (Gałuszka & Migaszewski, 2018).

Competing Interests

The authors declare no competing interests.

Supplementary Materials

Supplementary data to this article can be found online at https://doi.org/10.2478/mipo-2024-0001.

References

Bong, W. S. K., Matsumura, K., Yokoyama, K., & Nakai, I. (2010). Provenance study of early and middle bronze age pottery from Kaman-Kalehöyük, Turkey, by heavy mineral analysis and geochemical analysis of individual hornblende grains. *Journal of Archaeological Science*, *37*, 2165–2178. https://doi.org/10.1016/j.jas.2010.03.013

Cabała, J., & Teper, L. (2007). Metalliferous constituents of rhizosphere soils contaminated by Zn–Pb mining in Southern Poland. *Water, Air & Soil Pollution*, *178*, 351–362. https://doi.org/10.1007/s11270-006-9203-1

Carlson, W. R. (2016). *Heavy minerals in soils from the Athabasca basin and the implications for exploration geochemistry of uranium deposits at depth*. A thesis submitted to the Department of Geological Sciences and Geological Engineering Queen's University

Kingston, Ontario, Canada. http://hdl.handle.net/1974/15203

Cho, K. H., Jang, H., Hong, Y.-S., Kim, S. J., Basch, R. H., & Fash, J. W. (2008). The size effect of zircon particles on the friction characteristics of brake lining materials. *Wear*, *264*, 291–297. https://doi.org/10.1016/j.wear.2007.03.018

Chopin, E. I., & Alloway, B. J. (2007). Trace element partitioning and soil particle characterisation around mining and smelting areas at Tharsis, Ríotinto and Huelva, SW Spain. *Science of the Total Environment*, *373*(2–3), 488–500. https://doi.org/10.1016/j.scitotenv.2006.11.037

Ettler, V., Johan, Z., Kříbek, B., Veselovský, F., Mihaljevič, M., Vaněk, A., Penížek, V., Majer, V., Sracek, O., Mapani, B., Kamona, F., & NyambeEttler, V., Petráňová, V., Vítková, M., Mihaljevič, M., Šebek, O., & Kříbek, B. (2016). Reactivity of fly ash from copper smelters in an Oxisol: Implications for smelter-polluted soil systems in the tropics. *Journal of Soils Sediments*, *16*, 115–124. https://doi.org/10.1007/s11368-015-1174-7

Gałuszka, A., & Migaszewski, Z. M. (2018). Glass microspheres as a potential indicator of the Anthropocene: A first study in an urban environment. *The Holocene*, *28*(2), 323–329. https://doi.org/10.1177/0959683617721332

Hao, H., Guo, R., Gu, Q., & Hu, X. (2019). Machine learning application to automatically classify heavy minerals in river sand by using SEM/EDS data. *Minerals Engineering*, *143*, 105899. https://doi.org/10.1016/j.mineng.2019.105899

Hołtra, A., & Zamorska-Wojdyła, D. (2020). The pollution indices of trace elements in soils and plants close to the copper and zinc smelting works in Poland's Lower Silesia. *Environmental Science and Pollution Research*, *27*(14), 16086–16099. https://doi.org/10.1007/s11356-020-08072-0

Jagodziński, R., Sternal, B., Szczuciński, W., Chagué-Goff, C., & Sugawara, D. (2012). Heavy minerals in the 2011 Tohoku-oki tsunami deposits—insights into sediment sources and hydrodynamics. *Sedimentary Geology*, *282*, 57–64. https://doi.org/10.1016/j.sedgeo.2012.07.015

Jarošíková, A., Ettler, V., Mihaljevič, M., Penížek, V., Matoušek, T., Culka, A., & Drahota, P. (2018). Transformation of arsenic-rich copper smelter flue dust in contrasting soils: A 2-year field experiment. *Environmental Pollution*, *237*, 83–92. https://doi.org/10.1016/j.envpol.2018.02.028

Kacem, I., Gautron, L., Coillot, D., & Neuville, D. R. (2017). Structure and properties of lead silicate glasses and melts. *Chemical Geology*, *461*, 104–114. https://doi.org/10.1016/j.chemgeo.2017.03.030.hal-01632315

Karczewska, A., Kaszubkiewicz, J., Jezierski, P., Kabała, C., & Król, K. (2010). Level of soil contamination with copper, lead and cadmium within the protection zone of copper smelter Legnica in the years 1982 and 2005. *Roczniki Gleboznawcze*, *61*, 45–51. (in Polish with English summary)

KGHM Cuprum Sp.z.o.o. Research Center. Monograph of KGHM Polish copper company; KGHM Cuprum Sp.z.o.o. Research Center: Wrocław, Poland, 2007. (In Polish)

Khan, R., Das, S., Kabir, S., Habib, Md. A., Naher, K., Islam, M. A., Tamim, U., Rahman, A. K. M. R., Deb, A. K., & Hossain, S. M. (2019). Evaluation of the elemental distribution in soil samples collected from ship-breaking areas and an adjacent island. *Journal of Environmental Chemical Engineering*, *7*(3), 103189. https://doi.org/10.1016/j.jece.2019.103189

Lång, L. O. (2000). Heavy mineral weathering under acidic soil conditions. *Applied Geochemistry*, *15*(4), 415–423. https://doi.org/10.1016/S0883-2927(99)00064-5

Lanteigne, S., Schindler, M., & McDonald, A. M. (2014). Distribution of metals and metalloids in smelter-derived particulate matter in soils and mineralogical insights into their retention and release in a low-t environment. *The Canadian Mineralogist*, *52*(3), 453–471. https://doi.org/10.3749/canmin.52.3.453

Lanteigne, S., Schindler, M., McDonald, A. M., Skeries, K., Abdu, Y., Mantha, N. M., Murayama, M., Hawthorne, F. C., & Hochella, Jr., M. F. (2012). Mineralogy and weathering of smelter-derived spherical particles in soils: Implications for the mobility of Ni and Cu in the surficial environment. *Water, Air & Soil Pollution*, *223*, 3619–3641. https://doi.org/10.1007/s11270-012-1135-3

Li, X., Wu, L., Zhou, J., Luo, Y., Zhou, T., Li, Z., Hu, P., & Christie, P. (2022). Potential environmental risk of natural particulate cadmium and zinc in sphalerite- and smithsonite-spiked soils. *Journal of Hazardous Materials*, *429*, 128313, https://doi.org/10.1016/j.jhazmat.2022.128313

Lim, Y. C., Marolf, A., Estoppey, N., & Massonnet, G. (2021). A probabilistic approach towards source level inquiries for forensic soil examination based on mineral counts. *Forensic Science International*, *328*, 111035. https://doi.org/10.1016/j.forsciint.2021.111035

Lis, J., & Pasieczna, A. (2005). Anthropogenic soils pollution within the Legnica–Głogów copper district. *Polish Geological Institute Special Papers*, *17*, 42–48.

Mange, M. A., & Wright, D. T. (Eds.). (2007a). *Heavy minerals in use*. Elsevier. eBook ISBN: 9780080548593

Mange, M. A., & Wright, D. T. (2007b). High-resolution heavy mineral analysis (HRHMA): A brief summary. *Developments in Sedimentology*, *58*, 433–436. https://doi.org/10.1016/S0070-4571(07)58016-7

Matelski, R. P., & Turk, L. M. (1947). Heavy minerals in some podzol soil profiles in Michigan. *Soil Science*, *64*(6), 469–488.

Medyńska-Juraszek, A., & Kabała, C. (2012). Heavy metal pollution of forest soils affected by the copper industry. *Journal of Elementology*, *17*, 441–451. https://doi.org/10.5601/jelem.2012.17.3.07

Migaszewski, Z. M., Gałuszka, A., Dołęgowska, S., & Michalik, A. (2022). Abundance and fate of glass microspheres in river sediments and roadside soils: Lessons from the Świętokrzyskie region case study (south-central Poland). *Science of the Total Environment*, *821*, 153410. https://doi.org/10.1016/j.scitotenv.2022.153410

Morton, A. C. (1984). Stability of detrital heavy minerals in Tertiary Sandstones from the North Sea Basin. *Clay Minerals*, *19*, 287–308.

Morton, A. C. (1985). Heavy minerals in provenance studies. In *Provenance of arenites*, G. G. Zuffa (Ed.).

(pp. 249–277). Department of Earth Sciences, University of Calabria, Castiglione Cosentino Stazione, Cosenza, Italy: Springer Netherlands.

Pettijohn, F. J. (1941). Persistence of heavy minerals and geologic age. *The Journal of Geology*, *49*, 610–625.

Pietranik, A., Kierczak, J., Tyszka, R., & Schulz, B. (2018). Understanding heterogeneity of a slag-derived weathered material: The role of automated SEM-EDS analyses. *Minerals*, *8*, 513. https://doi.org/10.3390/min8110513

Potysz, A., Kierczak, J., Pietranik, A., & Kądziołka, K. (2018). Mineralogical, geochemical, and leaching study of historical Cu-slags issued from processing of the Zechstein formation (Old Copper Basin, Southwestern Poland). *Applied Geochemistry*, *98*, 22–35. https://doi.org/10.1016/j.apgeochem.2018.08.027

Razum, I., Rubinić, V., Miko, S., Ružičić, S., & Durn, G. (2023). Coherent provenance analysis of terra rossa from the northern Adriatic based on heavy mineral assemblages reveals the emerged Adriatic shelf as the main recurring source of siliciclastic material for their formation. *Catena*, *226*, 107083. https://doi.org/10.1016/j.catena.2023.107083

Stojanowska, A., Rybak, J., Bożym, M., Olszowski, T., & Bihałowicz, J. S. (2020). Spider webs and lichens as bioindicators of heavy metals: A comparison study in the vicinity of a copper smelter (Poland). *Sustainability*, *12*, 8066. https://doi.org/10.3390/su12198066

Strzelec, Ł., & Niedźwiecka, W. (2012). Stan środowiska naturalnego w rejonie oddziaływania hut miedzi. *Medycyna* Środowiskowa *Environmental Medicine*, *15*, 21–31. (in Polish)

Sulieman, M. M., Ibrahim, I. S., Elfaki, J. T., & Dafa-Allah, M. S. (2015). Origin and distribution of heavy minerals in the surficial and subsurficial sediments of the alluvial Nile river terraces. *Open Journal of Soil Science*, *5*, 299–310. https://doi.org/10.4236/ojss.2015.512028

Tangari, A. C., Le Pera, E., Andò, S., Garzanti, E., Piluso, E., Marinangeli, L., & Scarciglia, F. (2021). Soil-formation in the central Mediterranean: Insight from heavy minerals. *Catena*, *197*, 104998. https://doi.org/10.1016/j.catena.2020.104998

Tørseth, K., Aas, W., Breivik, K., Fjaeraa, A. M., Fiebig, M., Hjellbrekke, A. G., Lund Myhre, C., Solberg, S., & Yttri, K. E. (2012). Introduction to the European Monitoring and Evaluation Programme (EMEP) and observed atmospheric composition change during 1972–2009. *Atmospheric Chemistry and Physics*, *12*, 5447–5481. https://doi.org/10.5194/acp-12-5447-2012

Trzyna, A., Rybak, J., Bartz, W., & Górka, M. (2022). Health risk assessment in the vicinity of a copper smelter: Particulate matter collected on a spider web. *Mineralogia*, *53*, 36–50. https://doi.org/10.2478/mipo-2022-0004

Tuhý, M., Ettler, V., Rohovec, J., Matoušková, Š., Mihaljevič, M., Kříbek, B., & Mapani, B. (2021). Metal(loid)s remobilization and mineralogical transformations in smelter-polluted savanna soils under simulated wildfire conditions. *Journal of Environmental Management*, *293*, 112899. https://doi.org/10.1016/j.jenvman.2021.112899

Tuhý, M., Hrstka, T., & Ettler, V. (2020). Automated mineralogy for quantification and partitioning of metal(loid)s in particulates from mining/smelting-polluted soils. *Environmental Pollution*, *266*, 115118. https://doi.org/10.1016/j.envpol.2020.115118

Tyszka, R., Kierczak, J., Pietranik, A., Ettler, V., & Mihaljevič, M. (2014). Extensive weathering of zinc smelting slag in a heap in Upper Silesia (Poland): Potential environmental risks posed by mechanical disturbance of slag deposits. *Applied Geochemistry*, *40*, 70–81. https://doi.org/10.1016/j.apgeochem.2013.10.010

Tyszka, R., Pietranik, A., Kierczak, J., Ettler, V., Mihaljevič, M., & Medyńska-Juraszek, A. (2016). Lead isotopes and heavy minerals analyzed as tools to understand the distribution of lead and other potentially toxic elements in soils contaminated by Cu smelting (Legnica, Poland). *Environmental Science and Pollution Research*, *23*, 24350–24363. https://doi.org/10.1007/s11356-016-7655-4

Tyszka, R., Pietranik, A., Potysz, A., Kierczak, J., & Schultz, B. (2021). Experimental simulations of Zn-Pb slag weathering and its impact on the environment: Effects of acid rain, soil solution, and microbial activity. *Journal of Geochemical Exploration*, *228*, 106808. https://doi.org/10.1016/j.gexplo.2021.106808

Waroszewski, J., Pietranik, A., Sprafke, T., Kabała, C., Frechen, M., Jary, Z., Kot, A., Tsukamoto, S., Meyer-Heintz, S., Krawczyk, M., Łabaz, B., Schultz, B., & Erban-Kochergina, Y. V. (2021). Provenance and paleoenvironmental context of the Late Pleistocene thin aeolian silt mantles in southwestern Poland – A widespread parent material for soils. *Catena*, *204*, 1–13. https://doi.org/10.1016/j.catena.2021.105377

Yu, X., Wang, Y., & Lu, S. (2020). Tracking the magnetic carriers of heavy metals in contaminated soils based on X-ray microprobe techniques and wavelet transformation. *Journal of Hazardous Materials*, *382*, 121114. https://doi.org/10.1016/j.jhazmat.2019.121114